ISSN 2079-1704. Хімія, фізика та технологія поверхні. 2024. Т. 15. № 2. С. 212-220

PACS number: 61.46.Bc doi: 10.15407/hftp15.02.212

S.S. Kovachov, I.T. Bohdanov, D.S. Drozhcha, K.M. Tikhovod, V.V. Bondarenko, I.G. Kosogov, Ya.O. Suchikova

STUDY ON PHASE CHARACTERISTICS OF HETEROSTRUCTURE por-Ga_2O_3/GaAs

Berdyansk State Pedagogical University
4 Shmidta Str., Berdyansk, 71100, Ukraine, E-mail: yanasuchikova@gmail.com

The synthesis and characterization of heterostructure por-Ga_2O_3/GaAs represent a crucial advancement in nanomaterials, particularly in optoelectronic applications. Employing a two-stage electrochemical etching methodology, this research has elucidated the precise conditions required to fabricate such a heterostructure. The initial stage involves etching monocrystalline gallium arsenide (GaAs) using an aqueous nitric acid solution as the electrolyte. This process is governed by the redox reactions at the crystal-electrolyte interface, where GaAs are partially oxidized and selectively etched.

The second stage introduces ethanol into the electrolytic solution. This chemical addition serves a dual purpose: Firstly, it modulates the electrochemical environment, allowing for controlling pore morphology in GaAs. Secondly, it facilitates the etching of the resultant oxide layer, which predominantly consists of gallium oxide (Ga_2O_3). The formation of this oxide layer can be attributed to the oxidation of GaAs, driven by the electrochemical potentials and resulting in the deposition of reaction by-products on the substrate surface.

The fabricated nanocomposite was comprehensively characterized using Scanning Electron Microscopy (SEM), Energy Dispersive X-ray Analysis (EDX), and Raman Spectroscopy. SEM imaging revealed a range of agglomerated nanostructures dispersed across the surface, with dimensions ranging from 8–25 μm, 1–1.5 μm, and 70–100 nm. These observations suggest a hierarchical pore structure indicative of a complex etching mechanism modulated by the electrolyte composition.

Raman spectroscopic analysis corroborated the presence of various phases in the heterostructure. Signals corresponding to bulk GaAs, serving as the substrate, were distinguishable. In addition, peaks indicative of porous GaAs and porous Ga_2O_3 were observed. A cubic phase in the Ga_2O_3 layer was particularly noteworthy, suggesting a higher degree of crystallinity. Notably, the absence of Raman-active modes associated with internal stresses implies that the fabricated heterostructure is of high quality.

***Keywords**: Ga_2O_3, GaAs, electrochemical etching, oxidation, pores, heterostructures*

INTRODUCTION

The semiconductor β-Ga_2O_3 has attracted the attention of researchers due to its exceptional properties: wide bandgap (~ 4.9 eV) [1], high breakdown electric field (~ 8 $MV \cdot cm^{-1}$) [2], good radiation resistance [3], and compatibility of its crystal lattice with other wide band gap semiconductors [4, 5]. Various methods, including epitaxial growth [6, 7], thermal annealing [8, 9], and electrodeposition [10–12], are used to synthesize these semiconductors. Their functional applications [13, 14] are the main reason for interest in them.

Ga_2O_3 is used to create high-precision lasers for military applications [15, 16]. In particular, it has been shown in [17] that the wide band gap of beta-gallium oxide makes it an ideal material to detect ultraviolet radiation. In addition, its bandgap width leads to photon absorption edge at the blind sun regime's boundary wavelength, which can be used to track rocket trails, detect flames, and monitor the environment.

Scientists' efforts are focused on finding substrates for oxide semiconductors. The main problems in choosing substrates are poor adhesion of oxide layers and their delamination, mismatch of crystal lattices, which leads to excessive stresses at the junction, and uneven layer formation on the surface [18, 19]. In [20], Ga_2O_3 was synthesised on sapphire and silicon substrates by sublimation. The authors of [21] demonstrated that gallium oxide can be synthesised on diamond substrates. However, the authors emphasised the problems of growing high-quality Ga_2O_3/diamond heterostructures due to the mismatch of crystal lattice parameters, making direct growth impossible. In addition, the

© S.S. Kovachov, I.T. Bohdanov, D.S. Drozhcha, K.M. Tikhovod, V.V. Bondarenko, I.G. Kosogov, Ya.O. Suchikova, 2024

rough surface of diamond does not allow for a seamless contact at their hetero-interface.

This work investigates the conditions for the formation of nanostructured Ga_2O_3 on monocrystalline GaAs substrates using the electrochemical etching method.

MATERIALS AND RESEARCH METHODS

Samples for the experiment. Monocrystalline semi-conductor gallium arsenide plates grown by the Czochralski method were used to form Ga_2O_3 layers (Table). The type of the conductivity of crystals determines the dynamics and mechanisms of digestion. Thus, it is well known that A^3B^5 *p*-type semiconductors are etched without the formation of a porous layer; their surface has a textured morphology, while the *n*-type conductivity of crystals allows the formation of a dense ensemble of pores on the surface [22, 23]. This is because the required local concentration of holes can be created only if they are not the leading carriers, *i.e.,* in *n*-type semiconductor crystals. Under similar conditions of anodic polarisation, *p*-type semiconductors are etched uniformly or with the formation of textures on the surface. The set of plates with dimensions of 10×20×2 mm was used. The plates were polished on both sides to a mirror finish. Before the experiment, the samples were purified and degreased in acetone, ethyl alcohol, and deionized water.

Table. Samples for the experiment

Item	Specifications
Conductivity type	N-type
Dopant	Sb
Carrier concentration	2.3×10^{18} cm^{-3}
Orientation	(111)
Crystal lattice	face-centered cubic (“zinc blende”)
Lattice period	0.5653 nm
Atomic density	4.43×10^{22} cm^{-3}

Methods of synthesis of nanostructures. Electrochemical etching in acid solutions was chosen as the method for layer formation. This method is simple and inexpensive, making it attractive for producing semiconductors on a production scale [24]. The advantages of this method include the following electrochemical digestion in acid solutions, which allows for the high selectivity of electrochemical processes [25]. This is because the oxidation and reduction processes at the electrodes occur with the participation of electrons (there is no need to use complex chemical reagents and technologies). In addition, the electrochemical processes at the electrolyte/semiconductor interface are characterized by a slight change in potential when the anodizing current changes. This makes it easy to control the dissolution of the semiconductor directly during digestion.

At the same time, the electrochemical etching method has several disadvantages, including exfoliation of the substance from the surface of the anode, formation of pores in the structure of the deposited film, and formation of an intensely textured structure with the presence of needles, spikes, and whiskers on the surface. These can lead to potential gradients in the electric field [26, 27].

The applied potential causes a change in the morphology of the semiconductor surface, so it is possible to form a large number of unique structures with given properties [28, 29]. Electrochemical treatment of the semiconductor is characterized by the following processes: surface polishing (etching of surface micro defects); selective etching (formation of the porous or textured layer as a result of pulling atoms of material from the surface and entering the electrolyte), electrochemical deposition (formation on the surface of nano relief material due to the deposition of reaction products or oxidation of the crystal surface) [30]. These processes are competitive, but it is possible to implement them in parallel in one experiment [31]. In this study, por-Ga_2O_3/GaAs heterostructures were synthesized using a two-step electrochemical etching method.

Device for experiment. The experiment was performed in a three-electrode quartz electrolytic cell (Fig. 1). The electrodes were the silver

chloride reference electrode, platinum (cathode), and gallium arsenide plate (anode). The anode and cathode were parallel to each other and perpendicular to the bottom of the cell at a distance of 1 cm. Potentiostat MTech SPG-500S was used to monitor changes in the anodizing current. Based on the changes in the current values, conclusions were made about the stages of electrochemical etching. A Teflon stirrer was used to remove bubbles from the sample surface. The electrochemical cell blowing module was also used. The experiment was carried out under normal conditions and in daylight.

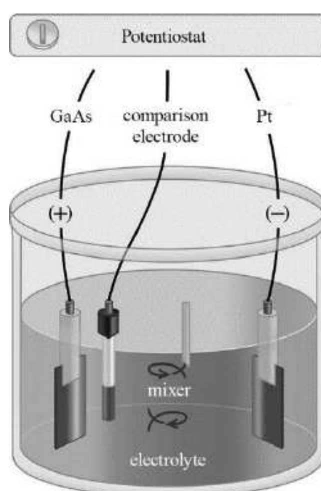

Fig. 1. Device for electrochemical etching of crystals

Preparation of the GaAs surface for forming Ga_2O_3. The experiment was carried out in two stages. The purpose of the first step was to form the textured (porous) layer on the surface of the monocrystalline gallium arsenide, which will later be a 'soft' substrate for the formation of gallium oxide. The aim of the second stage was the synthesis of Ga_2O_3.

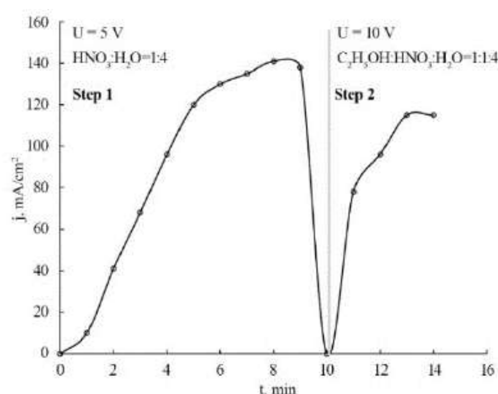

Fig. 2. Diagram characterizing the change in the value of current density over time during electrochemical etching of *n*-GaAs

The solution of nitric acid was used to implement the first stage. The acid concentration in the electrolyte, respectively, was $HNO_3 : H_2O = 1 : 4$. The DC voltage mode (U = 5V) was used. The processes of electrochemical dissolution of the crystals were recorded by removing the current. At this stage of digestion, a gradual increase in current was observed, which characterized the active electrochemical process of dissolving the semiconductor wafer (Fig. 2, step 1). Starting at 9 min of etching, the current began to fall intensely, indicating the completion of the electrochemical etching process and passivation of the sample surface with an oxide film. In this mode, the samples were etched for 10 min. After

that, the stage was completed. The solution was de-energized.

Synthesis of por-Ga_2O_3. To implement the second stage of the experiment, ethanol was added to the same solution. The ratio of components in the solution $C_2H_5OH : HNO_3 : H_2O = 1 : 1 : 4$. The samples were electrochemically etched using the same technology for 3 min. The DC voltage mode at U = 10V was used. Current values were recorded during etching. After 3 min of digestion, the current stopped growing, which indicated the completion of the active phase of the electrochemical process (Fig. 2, step 2). The electrolyte was de-energized. The samples were kept in solution for another 2 min without potential application. At the end of the experiment, the samples were washed in deionized water, dried under a stream of nitrogen, and left in the air for 1 month to check the chemical stability of the formed structure.

Research methods. As research methods, it was used:

– to study the micro and macromorphology of the surface of the synthesized heterostructure of scanning electron microscopy (SEO-SEM Inspect S50-B), the morphological parameters of nanostructures were evaluated using the ImageJ software product ImageJ;

– to study the component composition of the surface energy dispersion analysis EDX;

– for the study of the phase state and crystallinity of the obtained structures, as well as the identification of nanostructure surface materials, the Raman spectroscopy (RENISHAW inVia Reflex microspectrometer, 532 nm laser, 2400 nm grating, 100–1000 cm range, measurement time 10 s).

Before SEM, Raman, and EDX analyses, the samples were meticulously cleaned in deionized water to minimize organic or inorganic contamination. The objective was to ensure that the detected elements were intrinsic to the electrochemical processes, not artifacts from environmental exposure.

ImageJ and OriginPro software products were used to analyze the morphological characteristics of the surface.

RESULTS OF EXPERIMENTS AND DISCUSSION

SEM analysis. In Fig. 3 the work demonstrates the SEM image of the surface of the synthesized structure. Before SEM analysis, the samples were subjected to a mild surface cleaning using deionized water to remove possible organic residues, ensuring a clean surface for high-resolution imaging. One can see two areas with dense crater pores and areas with textured surfaces - in Fig. 3, they are marked (i) and (ii), respectively. Analysis of this image shows that the pores are more profound than the textured layer. From this, we can conclude that the textured layer was formed during the first etching stage and is a passivating film. For GaAs, such film is its oxides [32, 33]. During the second etching stage, etching of the upper layer is observed. The pores have a conical shape and significant scatter in diameter, from 8 to 25 microns. The nuclei of such massive pores are the defects of the crystal lattice, which are the predominant sites of the formation of pits of electrochemical etching.

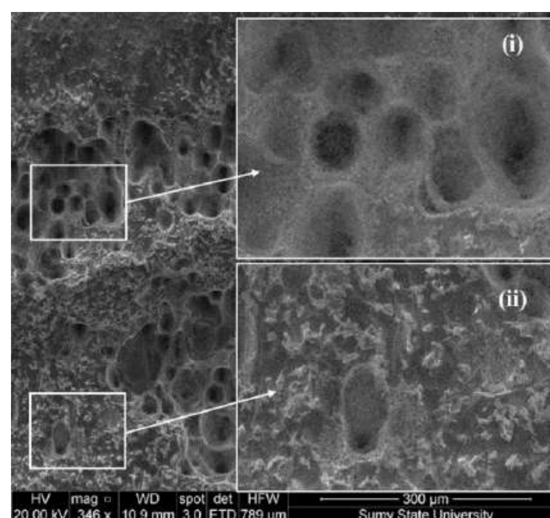

Fig. 3. SEM image of por-Ga_2O_3/por-GaAs/mono-GaAs surface

Fig. 4 shows the surface fragment, which shows the massive pore. One can see that its walls are loose and consist of tiny pores of two types. The first type of pore is located near the surface. These pores have a cross-sectional diameter 1–1.4 µm (Fig. 5 *a*). The second type of pore (2) can be observed near the bottom of the massive pore. Such pores have diameters in the range 100–200 nm (Fig. 5 *a*). That is, the formation of meso- and macropores is observed. The thickness of the interpore walls is 70–100 nm. These pores are densely packed and form a dense spongy structure. The porosity of the structure is 65 % (Fig. 5 *b*).

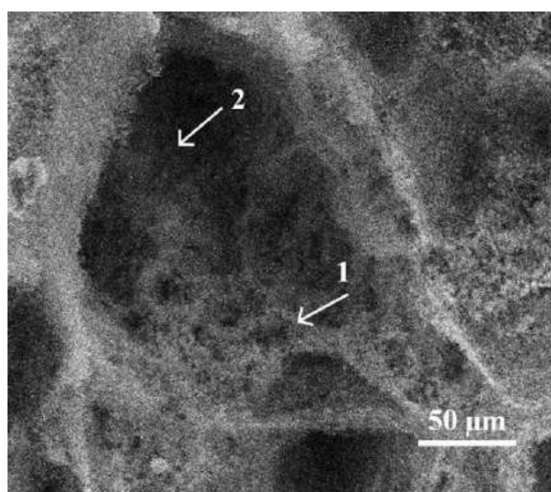

Fig. 4. Fragment of the morphology of the surface of the sample, showing the formation of pores inside the massive etching hole

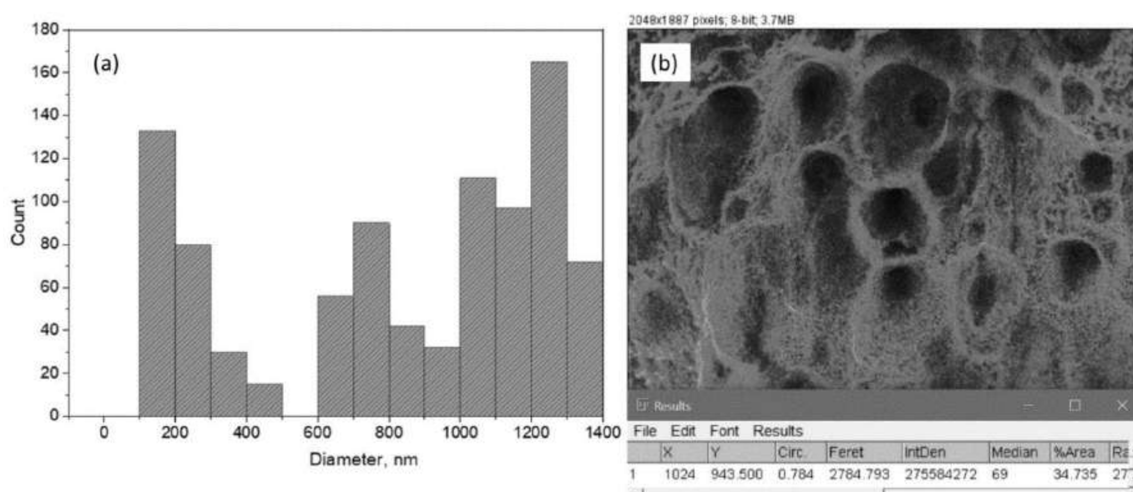

Fig. 5. Histogram of the distribution of pores by diameter (*a*) and calculation of the porosity of the surface of the synthesized structure using ImageJ software (*b*)

EDX mapping analysis. The component composition analysis of the samples obtained via EDX mapping indicates the presence of Ga, As, O, and C atoms on the crystal surface (Fig. 6). Oxygen appears on the surface as a result of oxidation of surface-unbound particles mainly during the etching process in the electrolyte. However, since the samples were exposed to air for an extended period post-synthesis (1 month), further oxidation in the air cannot be completely ruled out. The detected carbon could arise from two possible sources: the ethanol in the electrolyte solution or airborne contamination during post-synthetic exposure. Although carbon is present on the surface, its localized distribution and the nature of its presence suggest its unlikely significant impact on the overall electronic properties of the material. This is particularly due to its heterogeneous fact and the possible localized nature of its interaction with the material. For a more detailed understanding of the impact of carbon on electronic properties, additional characterization methods focused on studying the electronic structure are recommended.

Raman spectroscopy analysis. Research on Raman scattering of light shows the presence of peaks in the low-frequency region of the band (Fig. 7). The most intense spectrum at 191 cm^{-1} corresponds to the Ga_2O_3 spectrum. The shift

towards the low-frequency region of the spectrum relative to the typical Ga_2O_3 peak at 201 cm^{-1} [34, 35] indicates the presence of nanoparticles, as shown in the works [36, 37]. This is also confirmed by studies that observed small red and blue shifts in the combination scattering peaks due to internal deformation of nanowires [38].

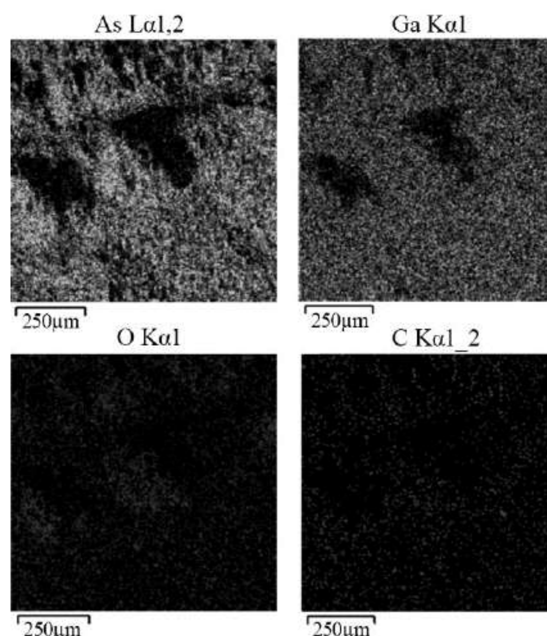

Fig. 6. EDX mapping analysis of por-Ga_2O_3/por-GaAs/mono-GaAs

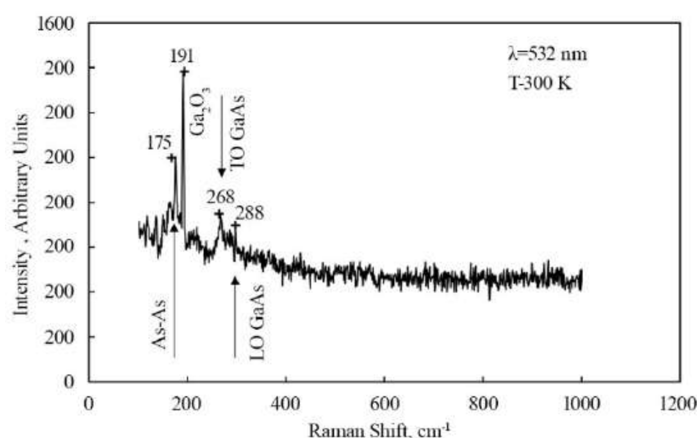

Fig. 7. Raman spectra of heterostructure por-Ga_2O_3/por-GaAs/mono-GaAs

This is also consistent with the results of scanning electron spectroscopy, demonstrated in Fig. 4. The half-width of this peak is 4 cm^{-1}. In work [39], it is shown that this may indicate the excellent crystallinity of the obtained films.

The peak at 268 cm^{-1} occurs due to scattering from the TO phonon, while the peak at 288 cm^{-1} occurs due to scattering from the LO phonon. The LO peak demonstrates a minimal full width at half maximum (FWHM), approximately 3 cm^{-1}. Peak positions correspond very well to the positions of TO and LO peaks measured in bulk (111) GaAs [40].

The measured values for the peak positions and FWHM indicate that the synthesized structures have good structural quality. This may also indicate the almost absence of stresses, which are usually present in bulk crystals due to the

presence of defects. Thus, in works [37–39, 41], it is shown that the presence of defects and stresses leads to a shift toward the red part of the spectrum, while the presence of nanoparticles may lead to a shift towards the blue part of the spectrum [39, 42], which corresponds well to our assumptions. Peaks located to the left of the Ga_2O_3 peak (191 cm^{-1}) may arise due to As-As vibrations.

Although other types of oxides have been reported multiple times that form on the surface of GaAs due to electrochemical treatment, peaks from their presence have not been detected [43, 44]. This is likely due to the instability of other native oxides, such as As_2O_3, especially in the aggressive environment of the electrolyte [45, 46].

CONCLUSIONS

We have demonstrated a simple method for the synthesis of the heterostructure consisting of porous layers of Ga_2O_3 on substrates of monocrystalline gallium arsenide. The structure was constructed by electrochemical etching. The results of scanning electron microscopy showed the formation of massive pores in crater with diameter of 8–25 μm, the surface of which is loose and contains macropores 1–1.4 μm and pores of nanometre size 100–200 nm. The structure has a high porosity index of about 65 %. The results of the study of Raman scattering show that the porous layer of Ga_2O_3 has good quality, does not contain stresses and is in the crystalline phase.

AKNOWLEDGEMENTS

The study was supported by the Ministry of Education and Science of Ukraine, namely No. 0122U000129, No. 0121U10942, No. 0123U100110. Yana Suchikova thankful for the support from COST Action CA20129 MultIChem.

Дизайн та дослідження фазових характеристик гетероструктури por-Ga_2O_3/por-GaAs/mono-GaAs

С.С. Ковачов, І.Т. Богданов, Д.С. Дрожча, К.М. Тиховод, В.В. Бондаренко, І.Г. Косогов, Я.О. Сичікова

Бердянський державний педагогічний університет
вул. Шмідта, 4, Бердянськ, 71100, Україна, yanasuchikova@gmail.com

Синтез і характеристика гетероструктури por-Ga_2O_3/GaAs являють вирішальний прогрес у галузі наноматеріалів, особливо в оптоелектронних застосуваннях. Використовуючи методологію двостадійного електрохімічного травлення, це дослідження з'ясувало точні умови, необхідні для виготовлення такої гетероструктури. Початковий етап включає травлення монокристалічного арсеніду галію (GaAs) з використанням водного розчину азотної кислоти як електроліту. Цей процес регулюється окисно-відновними реакціями на межі кристал-електроліт, де GaAs частково окиснюється та вибірково травиться.

На другому етапі в електролітичний розчин вводиться етанол. Ця хімічна добавка виконує подвійну роль: по-перше, вона модулює електрохімічне середовище, таким чином дозволяючи контролювати морфологію пор у GaAs. По-друге, це полегшує травлення отриманого оксидного шару, який переважно складається з оксиду галію (Ga_2O_3). Утворення цього оксидного шару можна пояснити окисненням GaAs, що викликається електрохімічними потенціалами та призводить до осадження побічних продуктів реакції на поверхні підкладки.

Вичерпну характеристику виготовленого нанокомпозиту було виконано з використанням скануючої електронної мікроскопії (SEM), енергетично-дисперсійного рентгенівського аналізу (EDX) і раманівської спектроскопії. SEM зображення виявило ряд агломерованих наноструктур, розсіяних по поверхні, з розмірами в діапазоні від 8–25, 1–1.5 мкм і 70–100 нм. Ці спостереження свідчать про ієрархічну структуру пор, що вказує на складний механізм травлення, який модулюється складом електроліту.

Раманівський спектроскопічний аналіз підтвердив наявність різних фаз у гетероструктурі. Сигнали, що відповідають об'ємному GaAs, який служить підкладкою, були чітко помітні. Крім того, спостерігалися піки, що вказують на пористий GaAs і пористий Ga_2O_3. Наявність кубічної фази в шарі Ga_2O_3 заслуговує особливої уваги, що свідчить про вищий ступінь кристалічності. Важливо, що відсутність Раманівських активних мод, пов'язаних із внутрішніми напругами, означає, що виготовлена гетероструктура має високу якість.

***Ключові слова**: Ga_2O_3, GaAs, електрохімічне травлення, оксидування, пори, гетероструктури*

REFERENCES

1. Wang Z., Cheng K., Sun J., Wang X., Wang G., Liu X., Ma X. Ultra-Wide Bandgap Quasi Two-Dimensional β-Ga_2O_3 with Highly In-Plane Anisotropy for Power Electronics. *Appl. Surf. Sci.* 2023. **619**: 156771.
2. Liu F., Zhao X., Li Y., Liu C. Photoluminescence properties and DFT simulations of the Cr ion-implanted (100)-oriented β-Ga_2O_3 single crystals. *J. Alloys Compd*. 2023. **946**: 169301.
3. Luchechko A., Vasyltsiv V., Kostyk L., Tsvetkova O., Popov A.I. Shallow and deep trap levels in X-ray irradiated β-Ga_2O_3: Mg. *Nucl. Instrum. Methods Phys. Res., Sect. B*. 2019. **441**: 12.
4. Suchikova Y., Lazarenko A., Kovachov S., Usseinov A., Karipbaev Z., Popov A.I. Formation of porous Ga_2O_3/GaAs layers for electronic devices. In: *2022 IEEE 16th International Conference on Advanced Trends in Radioelectronics, Telecommunications and Computer Engineering (TCSET).* (2022, February). IEEE. pp. 01–04.
5. Chiang Jung-Lung, Bharath Kumar Yadlapalli, Mu-I Chen, Dong-Sing Wuu. A Review on Gallium Oxide Materials from Solution Processes. *Nanomaterials*. 2022. **12**(20): 3601.
6. Miao Y., Liang B., Tian Y., Xiong T., Sun S., Chen C. Epitaxial growth of β-Ga_2O_3 nanowires from horizontal to obliquely upward evolution. *Vacuum.* 2021. **192**: 110444.
7. Tang X., Li K.H., Zhao Y., Sui Y., Liang H., Liu Z., Li X. Quasi-Epitaxial Growth of β-Ga_2O_3-Coated Wide Band Gap Semiconductor Tape for Flexible UV Photodetectors. *ACS Appl. Mater. Interfaces*. 2021. **14**(1): 1304.
8. Nakanishi M., Wong M.H., Yamaguchi T., Honda T., Higashiwaki M., Onuma T. Effect of thermal annealing on photoexcited carriers in nitrogen-ion-implanted β-Ga_2O_3 crystals detected by photocurrent measurement. *AIP Adv*. 2021. **11**(3): 035237.
9. Lee J., Kim H., Gautam L., He K., Hu X., Dravid V.P., Razeghi M. Study of phase transition in MOCVD grown Ga_2O_3 from κ to β phase by ex situ and in situ annealing. *Photonics*. 2021. **8**(1): 17.
10. Xie Y., Nie Y., Zheng Y., Luo Y., Zhang J., Yi Z., Wu P. The influence of β-Ga_2O_3 film thickness on the optoelectronic properties of β-Ga_2O_3@ ZnO nanocomposite heterogeneous materials. *Mater. Today Commun*. 2021. **29**: 102873.
11. Vequizo J.J.M.; Ichimura M. Electrodeposition of Ga-O Thin Films from Aqueous Gallium Sulfate Solutions. *Jpn. J. Appl. Phys.* 2013. **52**: 075503.
12. Vambol S.O., Bohdanov I.T., Vambol V.V., Onyschenko S.V. Formation of filamentary structures of oxide on the surface of monocrystalline gallium arsenide. *Journal of Nano-and Electronic Physics.* 2017. **9**(6): 06016.
13. Usseinov A., Koishybayeva Z., Akilbekov A., Abuova F.U., Kotomin E., Popov A.I. Ab initio calculations of native defects IN β-Ga_2O_3. *Latv. J. Phys. Tech. Sci*. 2021. **58**(2): 3.
14. Usseinov A., Platonenko A., Koishybayeva Z., Akilbekov A., Zdorovets M., Popov A.I. Pair vacancy defects in β-Ga_2O_3 crystal: Ab initio study. *Opt. Mater.: X.* 2022. **16**: 100200.
15. Lu Y.M., Li C., Chen X.H., Han S., Cao P.J., Jia F., Zhu D.L. Preparation of Ga_2O_3 thin film solar-blind photodetectors based on mixed-phase structure by pulsed laser deposition. *Chin. Phys. B*. 2019. **28**(1): 018504.
16. Yi G., Jeon S., Kwon Y.W., Park J., Nguyen D.A., Sandeep C.S., Kim Y.J. Enhanced third harmonic generation in ultrathin free-standing β-Ga_2O_3 nanomembranes: study on surface and bulk contribution. *Nanoscale*. 2022. **14**(1): 175.
17. Zheng X.Q., Xie Y., Lee J., Jia Z., Tao X., Feng P.X.L. Beta gallium oxide (β-Ga_2O_3) nanoelectromechanical transducer for dual-modality solar-blind ultraviolet light detection. *APL Mater*. 2019. **7**(2): 022523.
18. Kokubun Y., Miura K., Endo F., Nakagomi S. Sol-gel prepared β-Ga_2O_3 thin films for ultraviolet photodetectors. *Appl. Phys. Lett*. 2007. **90**: 2.
19. Sinha G., Ganguli D., Chaudhuri S. Crystallization and optical properties of finite sized β-Ga_2O_3 in sol-gel derived Ga_2O_3: SiO_2 nanocomposites. *J. Phys. Condens. Matter*. 2006. **18**: 11167.
20. Nikolaev V.I., Maslov V., Stepanov S.I., Bougrov V.E., Romanov A.E. Growth and characterization of β-Ga_2O_3 crystals. *J. Cryst. Growth*. 2017. **457**: 132.
21. Cheng Z., Wheeler V.D., Bai T., Shi J., Tadjer M.J., Feygelson T., Graham S. Integration of polycrystalline Ga_2O_3 on diamond for thermal management. *Appl. Phys. Lett*. 2020. **116**(6): 062105.
22. Sychikova Y.O., Bogdanov I.T., Kovachov S.S. Influence of current density of anodizing on the geometric characteristics of nanostructures synthesized on the surface of semiconductors of A^3B^5 group and silicon. *Funct. Mater*. 2019. **27**(1): 29.
23. Suchikova J.A., Kidalov V.V., Sukach G.A. Blue shift of photoluminescence spectrum of porous InP. *ECS Trans*. 2009. **25**(24): 59.
24. Sychikova Y.O. *Porous indium phosphide: Preparation and properties*. Handbook of Nanoelectrochemistry: Electrochemical Synthesis Methods, Properties, and Characterization Techniques. 2016. 283.
25. Suohikova Y., Vambol S., Vambol V., Mozaffari N., Mozaffari N. Justification of the most rational method for the nanostructures synthesis on the semiconductors surface. *J. Achiev. Mater. Manuf. Eng*. 2019. **92**(1–2), 19.

26. Kleimann P., Badel X., Linnros J. Toward the formation of three-dimensional nanostructures by electrochemical etching of silicon. *Appl. Phys. Lett*. 2005. **86**: 183108.
27. Yang X., Tong L., Wu L., Zhang B., Liao Z., Chen A., Zhou Y., Liu Y., Hu Y. Research progress of silicon nanostructures prepared by electrochemical etching based on galvanic cells. *J. Phys. Conf. Ser*. 2021. **2076**(1): 012117.
28. Zhang Y., Gao F., Wang D., Li Z., Wang X., Wang C., Du Y. Amorphous/crystalline heterostructure transition-metal-based catalysts for high-performance water splitting. *Coord. Chem. Rev*. 2023. **475**: 214916.
29. Yahaya M.Z., Nazeri M.F.M., Salleh N.A., Kurt A., Kheawhom S., Illés B., Mohamad A.A. Selective etching of lead-free solder alloys: A brief review. *Mater. Today Commun*. 2022. **33**: 104520.
30. Wang F., Wang X. Mechanisms in the solution growth of free-standing two-dimensional inorganic nanomaterials. *Nanoscale.* 2014. **6**(12): 6398.
31. Ogle K. Atomic emission spectroelectrochemistry: real-time rate measurements of dissolution, corrosion, and passivation. *Corrosion*. 2019. **75**(12): 1398.
32. Shiota I., Miyamoto N., Nishizawa J. Passivation of GaAs surfaces by GaO_xN_y films and by multilayers. *Surf. Sci*. 1979. **86**: 272.
33. Kwo J., Murphy D.W., Hong M., Opila R.L., Mannaerts J.P., Sergent A.M., Masaitis R.L. Passivation of GaAs using $(Ga_2O_3)_{1-x}(Gd_2O_3)_x$, $0 \leqslant x \leqslant 1.0$ films. *Appl. Phys. Lett*. 1999. **75**: 1116.
34. Dohy D., Lucazeau G., Revcolevschi A. Raman spectra and valence force field of single-crystalline β-Ga_2O_3 *J. Solid State Chem*. 1982. **45**: 180.
35. Kranert C., Sturm C., Schmidt-Grund R., Grundmann M. Raman tensor elements of β-Ga_2O_3. *Sci. Rep.* 2016. **6**(1): 1.
36. Gao Y.H., Bando Y., Sato T., Zhang Y.F., Gao X.Q. Synthesis, Raman scattering and defects of β-Ga_2O_3 nanorods. *Appl. Phys. Lett*. 2002. **81**(12): 2267.
37. Rao R., Rao A.M., Xu B., Dong J., Sharma S., Sunkara M.K. Blueshifted Raman Scattering and its Correlation with the [110] Growth Direction in Gallium Oxide Nanowires. *J. Appl. Phys*. 2005. **98**: 094312.
38. Yadav A., Fu B., Bonvicini S.N., Ly L.Q., Jia Z., Shi Y. β-Ga_2O_3 Nanostructures: Chemical Vapor Deposition Growth Using Thermally Dewetted Au Nanoparticles as Catalyst and Characterization. *Nanomaterials (Basel*). 2022. **12**(15): 2589.
39. Dohy D., Lucazeau G., Revcolevschi A. Raman spectra and valence force field of single-crystalline β Ga_2O_3. *J. Solid State Chem*. 1982. **45**: 180.
40. Ochoa M.A., Maslar J.E., Bennett H.S. Extracting electron densities in n-type GaAs from Raman spectra: Comparisons with Hall measurements. *J. Appl. Phys*. 2020. **128**(7): 10.1063.
41. Hosein I.D., Hegde M., Jones P.D., Chirmanov V., Radovanovic P.V. Evolution of the Faceting, Morphology and Aspect Ratio of Gallium Oxide Nanowires Grown by Vapor-solid Deposition. *J. Cryst. Growth*. 2014. **396**: 24.
42. Onuma T., Fujioka S., Yamaguchi T., Itoh Y., Higashiwaki M., Sasaki K., Masui T., Honda T. Polarized Raman spectra in β-Ga_2O_3 single crystals. *J. Cryst. Growth*. 2014. **401**: 330.
43. Suchikova Y., Kovachov S., Bohdanov I. Formation of oxide crystallites on the porous GaAs surface by electrochemical deposition. *Nanomaterials and Nanotechnology*. 2022. **12**(30): 184798042211273.
44. Brooks G.A., Rankin W.J. Solid-solution formation between arsenic and antimony oxides. *Metallurgical Mater Trans B*. 1994. **25**(6): 865.
45. Mikoushkin V.M., Bryzgalov V.V., Nikonov S.Y. Composition and band structure of the native oxide nanolayer on the ion beam treated surface of the GaAs wafer. *Semiconductors.* 2018. **52**(5): 593.
46. Quagliano L.G. Detection of As_2O_3 arsenic oxide on GaAs surface by Raman scattering. *Appl. Surf. Sci*. 2000. **153**(4): 240.

Надійшла 12.02.2023, прийнята 27.05.2024